Cell, Vol. 112, 303–315, February 7, 2003, Copyright ©2003 by Cell Press

TGF-β Signaling Activates Steroid Hormone Receptor Expression during Neuronal Remodeling in the *Drosophila* Brain

Xiaoyan Zheng,[1,5] Jian Wang,[1,5] Theodor E. Haerry,[3,5] Ann Y.-H. Wu,[1] Josephine Martin,[3,4] Michael B. O'Connor,[3,4] Ching-Hsien J. Lee,[2] and Tzumin Lee[1,*]

[1]Department of Cell and Structural Biology
University of Illinois
Urbana, Illinois 61801

[2]Section of Hematology/Oncology
Department of Internal Medicine
University of Illinois
Chicago, Illinois 60612

[3]Department of Genetics, Cell Biology, and Development

[4]Howard Hughes Medical Institute
University of Minnesota
Minneapolis, Minnesota 55455

Summary

Metamorphosis of the *Drosophila* brain involves pruning of many larval-specific dendrites and axons followed by outgrowth of adult-specific processes. From a genetic mosaic screen, we recovered two independent mutations that block neuronal remodeling in the mushroom bodies (MBs). These phenotypically indistinguishable mutations affect Baboon function, a *Drosophila* TGF-β/activin type I receptor, and dSmad2, its downstream transcriptional effector. We also show that Punt and Wit, two type II receptors, act redundantly in this process. In addition, knocking out dActivin around the mid-third instar stage interferes with remodeling. Binding of the insect steroid hormone ecdysone to distinct ecdysone receptor isoforms induces different metamorphic responses in various larval tissues. Interestingly, expression of the ecdysone receptor B1 isoform (EcR-B1) is reduced in activin pathway mutants, and restoring EcR-B1 expression significantly rescues remodeling defects. We conclude that the *Drosophila* Activin signaling pathway mediates neuronal remodeling in part by regulating EcR-B1 expression.

Introduction

Functional neural circuits are highly plastic, but very little is known about the molecular mechanisms that govern changes of neuronal connections in intact brains. Like most developmental processes, plasticity of neural circuits appears to be regulated both temporally and spatially. For instance, developing brains demonstrate far more prominent plasticity in neuronal connections than adult brains (reviewed in Murakami et al., 1992). In addition, activity-dependent refinement of vocal-controlling neural circuits occurs in the brains of juvenile songbirds during the sensitive period for song learning (Iyengar and Bottjer, 2002). Understanding the genetic programs that control neuronal plasticity may help develop strategies for manipulating neuronal connections in functional neural circuits.

Reorganization of neuronal connections involves elimination of subsets of existing neurites and/or elaboration of new processes (e.g., Levine, 1984). Such changes in neuronal projections are commonly observed during development, since neurons often send out exuberant processes in early stages and later undergo selective pruning to eliminate extra branches (Hubel et al., 1977; O'Leary and Koester, 1993). Holometabolous insects, which undergo complete metamorphosis, offer a convenient model system for studying neuronal remodeling. During metamorphosis, most neurons constituting the larval neural circuits undergo extensive remodeling in order to acquire the adult pattern of projections (Truman, 1990). Such remodeling of neuronal projections is essential for transformation of the larval mushroom bodies (MBs) to the adult MBs (Technau and Heisenberg, 1982; Lee et al., 1999), the olfactory learning and memory center in insects (e.g., de Belle and Heisenberg, 1994). In the larval brain, every MB neuron extends a single process from which dendrites branch out into the calyx (arrowhead in Figure 1A). The axon extends further and then bifurcates into two major branches, one projecting medially and the other projecting dorsally (arrows in Figure 1A). MB neurons generated prior to the mid-third instar stage, named γ neurons, prune their medial and dorsal branches during early metamorphosis (Figure 1B) and subsequently project axons only into the medial γ lobe of the adult MB (arrow in Figure 1C). Existing dendrites are also pruned in the remodeling neurons (Figure 1B, compared with Figure 1A). In contrast, the α′/β′ MB neurons that are born after the mid-third instar stage retain their larval projections during metamorphosis (data not shown; Lee et al., 1999).

The steroid molting hormone 20-hydroxyecdysone (hereafter referred to as ecdysone) is well implicated in regulating insect neuronal remodeling (reviewed in Levine et al., 1995). Studies from *Drosophila* demonstrate that binding of ecdysone to heterodimeric receptors, composed of the nuclear receptor superfamily members ecdysone receptor (EcR) and Ultraspiracle (USP; the *Drosophila* RXR) (Yao et al., 1992, 1993; Thomas et al., 1993), mediates diverse ecdysone-dependent biological activities via transcriptional regulatory hierarchies (reviewed in Thummel, 1996). There are three distinct isoforms of the ecdysone receptor, EcR-A, EcR-B1, and EcR-B2, that share common DNA binding and hormone binding domains but differ in the N-terminal portion (Talbot et al., 1993). Interestingly, *Drosophila* tissues with different metamorphic responses to ecdysone express different EcR isoforms (Talbot et al., 1993). Consistent with the notion that EcR-B1 is specifically involved in remodeling of larval cells (Bender et al., 1997; Truman et al., 1994), EcR-B1 is abundantly present in the remodeling MB γ neurons but absent in α′/β′ neurons (Lee et al., 2000a). Elucidating how EcR-B1 expression is controlled should shed new

*Correspondence: tzumin@life.uiuc.edu

[5]These authors contributed equally to this work.

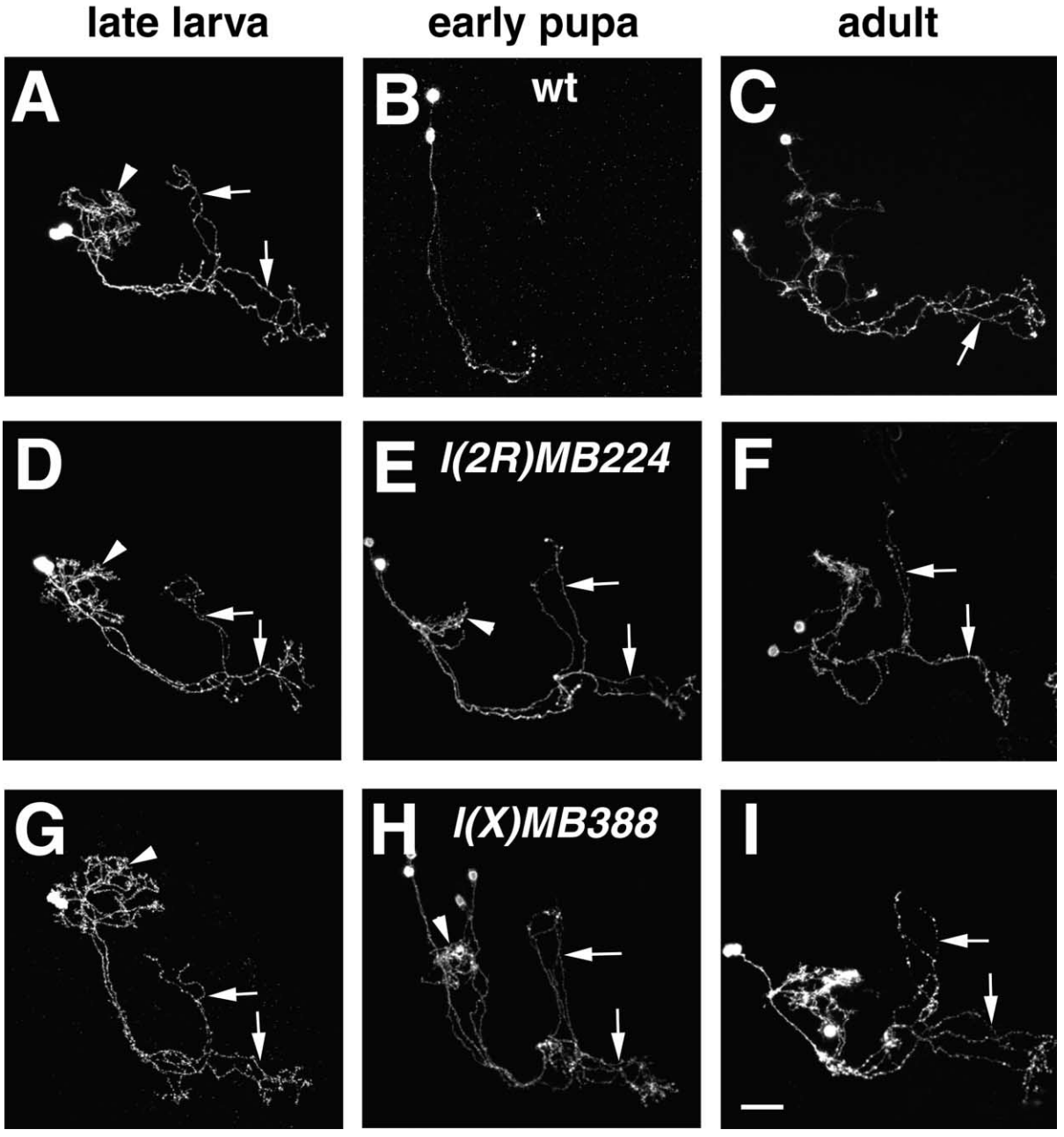

Figure 1. MB γ Neurons that Are Homozygous for the *l(2R)MB224* or *l(X)MB388* Mutation Retain Larval-Stage Dendrites and Axonal Branches through Metamorphosis

Two-cell/single-cell clones of MB γ neurons that are wild-type (A–C), homozygous for *l(2R)MB224* (D–F), or homozygous for *l(X)MB388* (G–I) were generated in newly hatched larvae and then examined at the wandering larval (A, D, and G), early pupal (B, E, and H), or adult stages (C, F, and I). Note that mutant γ neurons retain larval-type axon projection patterns and extend their axonal branches both dorsally and medially in adult brains (arrows in [F] and [I]). Dendrites and major axonal branches are indicated by arrowheads and arrows, respectively.
Genotype: (A–C) *hs-FLP/X;FRTG13,UAS-mCD8-GFP,GAL4-201Y/FRTG13,tubP-GAL80*; (D–F) *hs-FLP/X;FRTG13,l(2R)MB224,UAS-mCD8-GFP,GA4-201Y/FRTG13,tubP-GAL80*; (G–I) *FRT19A,l(X)MB388,UAS-mCD8-GFP/FRT19A,tubP-GAL80,hs-FLP;GAL4-201Y/+*.
The scale bar in this and all figures (unless otherwise indicated) equals 20 μm. All unilateral MB clones are oriented such that their processes extend from left to right toward the midline. All images are processed from composite confocal images, unless otherwise indicated.

light on the genetic programs governing neuronal plasticity.

Using MB γ neurons as a genetic model system, we have been investigating the molecular mechanisms of neuronal remodeling by conducting forward genetic mosaic screens (Lee et al., 2000a; Wang et al., 2002). The recently established MARCM system has allowed us to generate specifically labeled clones of MB neurons that are homozygous for a random mutation (Lee and Luo, 1999; Lee et al., 2000b; reviewed in Lee and Luo, 2001).

We reasoned that if a gene is required in MB γ neurons for pruning their larval-specific axons, the loss of such a gene in MB γ neurons would be expected to result in a phenotype in which adult γ neurons retain the larval dorsal branches (e.g., Figures 1F and 1I). Based on this readily discernible phenotype, we identified two additional independent mutations after recovering a *usp* mutation from our previous screen (Lee et al., 2000a). Phenotypic analysis through different developmental stages reveals that remodeling of MB γ neurons is completely blocked in these two phenotypically indistinguishable mutants. Moreover, we find that EcR-B1 expression is drastically suppressed in the mutant γ neurons and that restoration of EcR-B1 expression significantly rescues their remodeling defects. Mapping by recombination and complementation confirms that one of the two mutants is allelic to *baboon* (*babo*), the *Drosophila* TGF-β/Activin type I receptor. Interestingly, the other mutation is found to reside in the *dSmad2*, a gene encoding a well-known substrate for the Babo serine/threonine protein kinase (Brummel et al., 1999; Das et al., 1999). Furthermore, we also demonstrate that the two *Drosophila* type II receptors, Wit and Punt, act redundantly in this process. We also show that knocking out dActivin blocks EcR-B1 expression in the late third instar larval brain. Taken together with other experimental results, we conclude that the Babo/dSmad2-mediated TGF-β/Activin signaling mediates remodeling of MB neurons via controlling EcR-B1 expression.

Results

Two Independent Mutations, *l(2R)MB224* and *l(X)MB388*, Block Remodeling of the MB γ Neurons

Using MARCM, we have been screening for mutations that disrupt normal development of the MBs by creating and examining clones of homozygous mutant MB neurons in otherwise phenotypically wild-type organisms (Lee et al., 2000a; Wang et al., 2002). Prompted by our interests in remodeling of the MB γ neurons, we searched for two-cell/single-cell clones of mutant γ neurons that retained larval-specific projection patterns in adult brains. In wild-type organisms, all adult MB γ neurons project their axons medially toward the midline and lack dorsal-projecting axonal branches (Figure 1C). Among one thousand lethal mutations, *l(2R)MB224* and *l(X)MB388* cause indistinguishable, abnormal axon projection patterns in adult γ neurons. In both *l(2R)MB224* and *l(X)MB388* heterozygous adults, all two-cell/single-cell clones of homozygous mutant γ neurons possess two major axonal branches that project perpendicularly away from each other (arrows in Figures 1F and 1I; n = 100), as in larval γ neuron projections.

To check whether such abnormal axon projection patterns are acquired as a result of defects in remodeling of γ neurons during metamorphosis, we examined mutant neurons through different developmental stages. Since indistinguishable phenotypes are always observed in the *l(2R)MB224* and *l(X)MB388* lines, all the MARCM clones that are created in these two lines will be simply referred to as mutant neurons unless otherwise specified. In summary, we observe wild-type patterns of dendrites and axons in mutant γ neurons before puparium formation (PF) (Figures 1D and 1G). However, pruning of the larval dendrites and axons does not happen to mutant neurons during early metamorphosis. By 18 hr after PF, larval-specific axonal branches and most dendrites have been pruned in wild-type γ neurons (Figure 1B). In contrast, mutant γ neurons retain larval dendrites and axonal branches throughout metamorphosis (Figures 1E and 1H; data not shown). These observations indicate that the larval axon projection pattern persists in the adult *l(2R)MB224* and *l(X)MB388* mutant γ neurons due to a failure in pruning of larval-specific processes.

l(2R)MB224 Hinders MB Remodeling Due to a Loss-of-Function Mutation in the *babo* Gene

In order to identify the mutation that is responsible for blocking neuronal remodeling in the *l(2R)MB224* line, we first mapped a lethal mutation to the 44D–44F cytogenomic region based on complementation with the 2R deficiency kit (see Experimental Procedures). Further complementation assays using additional deficiency lines mapped the lethal mutation to the 44F11 region, where *flz* and *babo*, two previously identified lethal complementation groups, have been shown to reside (Figure 2A) (Konev et al., 1994; Dockendorff et al., 2000). Crossing with existing mutations revealed that the *l(2R)MB224* mutation failed to complement with several *babo* loss-of-function alleles. *babo* encodes a TGF-β/Activin type I receptor (Brummel et al., 1999). In addition, we observed enlarged anal pads that are characteristic of *babo* mutants in *l(2R)MB224* homozygous mutant larvae (data not shown), consistent with the notion that the *l(2R)MB224* is a *babo* mutant ($babo^{9}$).

To demonstrate that *l(2R)MB224* blocks remodeling of γ neurons purely due to a lethal *babo* mutation, we repeated the mosaic analysis using two independent *babo* null alleles, $babo^{52}$ (Brummel et al., 1999) and $babo^{Fd4}$ (see Experimental Procedures), and tried to rescue *l(2R)MB224* mutant phenotypes by expression of a wild-type *babo* cDNA. Larval-type projections persist in about 50% of $babo^{52}$ mutant γ neurons and 100% of $babo^{Fd4}$ mutant neurons (e.g., Figure 2B; n = 50), confirming that the TGF-β/Activin type I receptor Babo is required for pruning of larval-specific processes during metamorphosis. Given that persistence of larval-type projections is observed in all *l(2R)MB224* and $babo^{Fd4}$ mutant γ neurons, but only 50% of the $babo^{52}$ clones, a known null allele, we sequenced the $babo^{Fd4}$ allele. We find that the lesion involves a small deletion and addition at the last splice donor site (see Experimental Procedures). If splicing does not occur, this will lead to loss of the distal part of the kinase domain due to a stop codon within the intron. Such a mutation might be stronger than the null since it could potentially make a receptor that is still capable of binding ligands, but not signaling. If the Babo protein normally perdures for some time after clone induction, then the $babo^{Fd4}$ is likely to exhibit a stronger phenotype as a result of its antimorphic character.

As additional support for the notion that the remodeling defects are a direct result of loss of Babo function, we find that *l(2R)MB224* mutant neurons are completely rescued with respect to both dendritic elaboration and

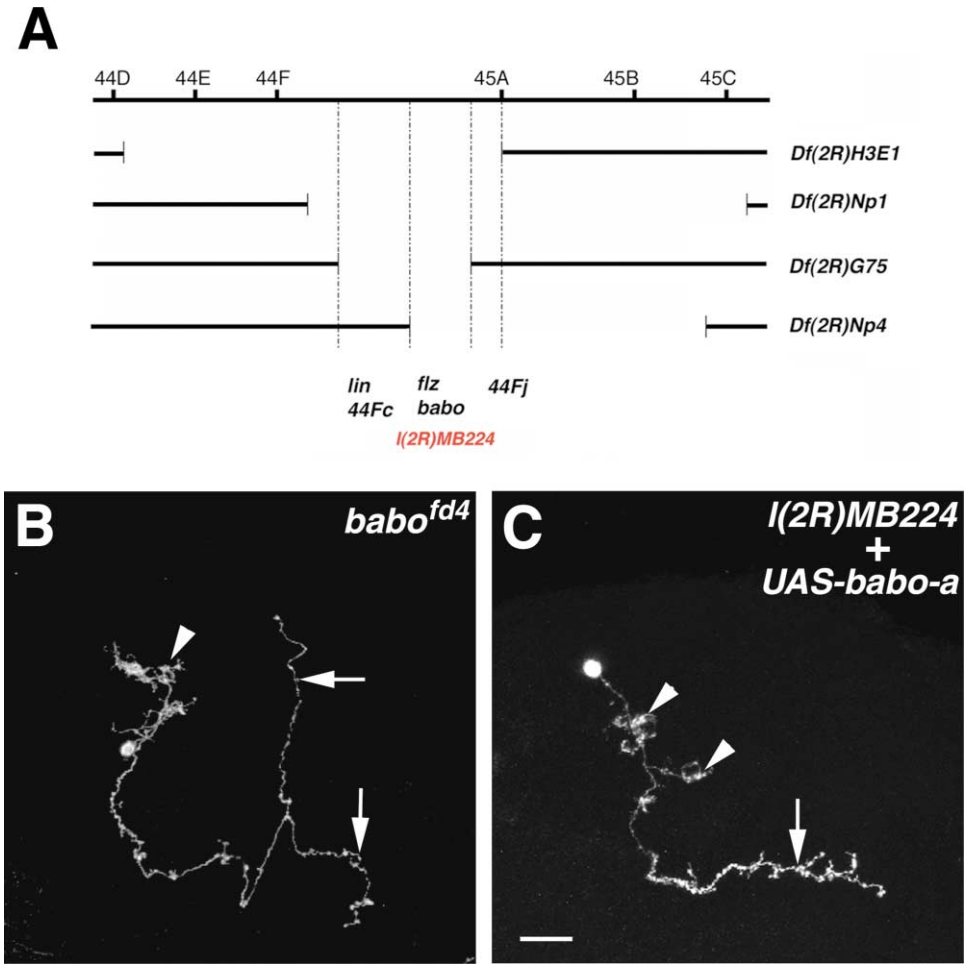

Figure 2. Mutations in the *babo* Gene, including *l(2R)MB224* (*babo*^{9}), Block MB Neuronal Remodeling and Expression of a Wild-Type *babo* cDNA Rescues Such Remodeling Defects

(A) *l(2R)MB224* carries a lethal mutation within the interval that is defined by the *Df(2R)Np4* proximal breaking point and the *Df(2R)G75* distal breaking point, given that *l(2R)MB224* failed to complement with all the listed deficiency lines.

(B) Larval-type dendrites (arrowheads) and axonal branches (arrows) persisted in an adult *babo*^{Fd4} homozygous γ neuron.

(C) In contrast, a *l(2R)MB224* mutant γ neuron acquired well-separated dendritic branches (arrowheads) and extended its only axonal process (arrow) medially toward the midline, after expression of a wild-type *babo* cDNA.

Genotype: (B) *UAS-mCD8-GFP,hs-FLP/X;FRTG13,babo[Fd4]/FRTG13,tubP-GAL80;GAL4-OK107/+*; (C) *hs-FLP/UAS-babo-a;FRTG13,l(2R)MB224,UAS-mCD8-GFP,GAL4-201Y/FRTG13,tubP-GAL80*.

axonal projections after driving expression of a wild-type *babo* cDNA specifically in the mutant neurons (Figure 2C; n = 50). Taken together, these results demonstrate that loss of Babo activity blocks remodeling of the MB γ neurons during metamorphosis.

l(X)MB388 Carries a Missense Mutation in the *dSmad2* Gene that Results in MB Remodeling Defects

In parallel experiments, we meiotically mapped the *l(X)MB388* mutation to the 7–8 cytogenomic region of the X chromosome (see Experimental Procedures). We confirmed and refined this location to the cytogenomic region between 7A and 8A by using a translocated X chromosome fragment. Mapping by complementation was then greatly facilitated using *l(X)MB388* hemizygous rescued male flies. Ultimately, we mapped the *l(X)MB388* mutation to the 7D10–7D12 region (Figure 3A). Interestingly, the *dSmad2* gene resides within this interval (Henderson and Andrew, 1998). The Smad family of proteins has been shown to mediate TGF-β signaling from the transmembrane TGF-β receptors to the nucleus (Heldin et al., 1997), in species ranging from worms to mammals (reviewed in Raftery and Sutherland, 1999; Massague and Chen, 2000; Savage-Dunn, 2001). dSmad2, which is most closely related to vertebrate Smads 2 and 3, is a known substrate for the Babo serine/threonine protein kinase in cultured cells (Brummel et al., 1999; Das et al., 1999).

Given that remodeling of γ neurons depends on Babo activity, we wondered whether a mutation in the Babo downstream effector dSmad2 blocks neuronal remodeling in the *l(X)MB388* line. The entire *dSmad2* genomic region was PCR amplified from both wild-type and mutant organisms. Sequence analysis of multiple independent PCR products demonstrated that the *l(X)MB388* chromosome has a missense mutation that results in

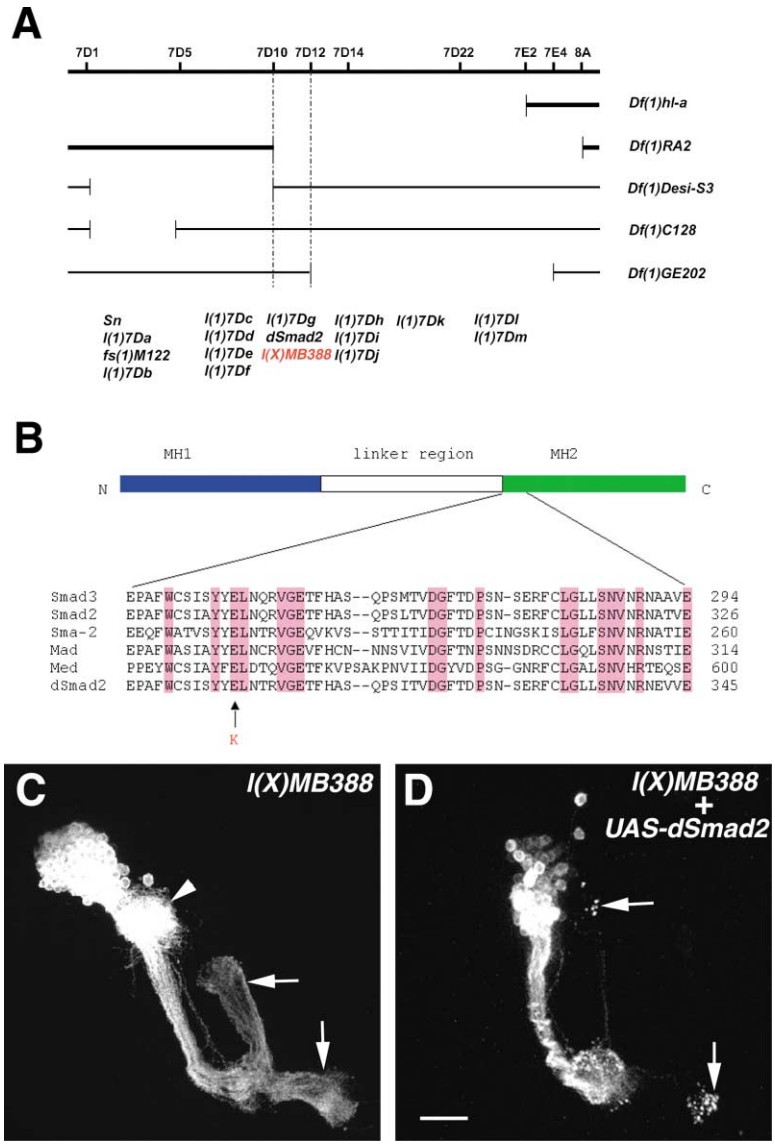

Figure 3. *l(X)MB388* (*dSmad2*^{1}) Carries a Missense Mutation in the *dSmad2* Gene, and Expression of a Wild-Type *dSmad2* cDNA Rescues Neuronal Remodeling Defects in *l(X)MB388* Mutant MB Neurons

(A) *l(X)MB388* failed to complement with the deficiency lines whose deficiency regions are indicated by gaps in thick lines but complemented with the deficiency lines whose deficiency regions are indicated by gaps in thin lines.

(B) Sequence alignment of part of the MH2 domain among Smad3, Smad2, Sma-2, Mad, Medea, and dSmad2. Well-conserved amino acids are shaded in pink. *l(X)MB388* carries a missense mutation in the *dSmad2* gene that changes one invariant glutamic acid to lysine.

(C) Larval calyx (arrowhead) and axonal bundles (arrows) persisted in a MB Nb clone of *l(X)388* mutant neurons when examined around 18 hr after puparium formation.

(D) In contrast, after expressing wild-type dSmad2 in a *l(X)MB388* mutant Nb clone, both calyx and larval axonal bundles were pruned by 18 hr after puparium formation. Note some axon debris (arrows) at tips of the pruned bundles.

Genotype: (C) *FRT19A,l(X)MB388,UAS-mCD8-GFP/FRT19A,tubP-GAL80,hs-FLP;GAL4-201Y/+*; (D) *FRT19A,l(X)MB388,UAS-mCD8-GFP/FRT19A,tubP-GAL80,hs-FLP;GAL4-201Y/+;UAS-dSmad2/+*.

replacement of Glu^{300} with Lys in the MH2 domain of the dSmad2 protein (Figure 3B). Most Smad proteins consist of two unrelated homology domains, the N-terminal MH1 and the C-terminal MH2 domains, which are separated by a variable linker region. In addition to containing a C-terminal SSXS motif for phosphorylation by TGF-β type I receptors, the MH2 domain is involved in mediating Smad-type I receptor binding, interaction with transcription factors, and oligomerization among Smads (reviewed in Massague, 1998). Interestingly, mutations in certain Smad proteins have been found in various cancers, and the majority of these tumor-derived missense mutations are clustered within the MH2 domain (Wu et al., 2001), including the same Glutamic acid to lysine change found in the *l(X)MB388*. These observations imply that dSmad2 function is compromised in the *l(X)MB388* mutant.

To determine whether *l(X)MB388* blocks neuronal remodeling due to loss of dSmad2 function, we tried to rescue *l(X)MB388* remodeling defects using a wild-type *dSmad2* cDNA. When a clone of *l(X)MB388* mutant γ neurons was examined around 18 hr after puparium formation, we observed persistence of larval-type bifurcated axon bundles as well as numerous dendritic branches, indicating no pruning of larval-specific processes (Figure 3C). In contrast, we observed that both larval-specific dendrites and axonal branches were completely pruned in *l(X)MB388* mutant γ neurons when a wild-type *dSmad2* cDNA was specifically expressed in the *l(X)MB388* mutant neurons (Figure 3D). In addition, ubiquitous expression of dSmad2 with an arm>GAL4 driver rescues the *l(X)MB388* mutation to viability, suggesting that no other lethal mutation resides on this chromosome. These results demonstrate that the Glu^{300} to Lys missense mutation in the *dSmad2* gene is responsible for blocking neuronal remodeling in the *l(X)MB388* (*dSmad2*^{1}) mutant line.

Expression of the EcR-B1 Isoform in Remodeling Neurons Depends on the Babo/dSmad2 Signaling Pathway

One key function of Smad proteins is regulation of gene expression in response to TGF-β signals (reviewed in Derynck et al., 1998). In order to elucidate how the Babo/

dSmad2 signaling pathway mediates neuronal remodeling via transcriptional regulation, we searched for dSmad2 target genes in remodeling neurons and found that expression of the EcR-B1 is much reduced in *babo/dSmad2* mutant γ neurons.

MARCM clones of *babo/dSmad2* mutant γ neurons were generated in newly hatched larvae and then examined for expression of EcR-B1 at the wandering larval stage. In the absence of MARCM clones, we observe four distinct clusters of tightly packed EcR-B1-positive nuclei in the region of MB cell bodies within each brain lobe (data not shown). By contrast, EcR-B1-negative holes are observed in the MB cell body regions that contain MARCM-labeled clones of *babo/dSmad2* mutant neurons. Examining EcR-B1 expression with single-nucleus resolution demonstrated that all *babo/dSmad2* mutant γ neurons, no matter whether they are present in big Nb clones or exist as isolated two-cell/single-cell clones, lack detectable EcR-B1 expression (Figures 4A–4D). In contrast, surrounding wild-type neurons are strongly positive for EcR-B1 (Figures 4A–4D). Furthermore, we observe rescue of EcR-B1 expression when the wild-type *babo* and *dSmad2* cDNAs were expressed in the *babo* and *dSmad2* mutant clones, respectively (Figures 4E and 4F; data not shown). These results indicate that high-level expression of EcR-B1 in remodeling neurons depends on normal Babo/dSmad2 activity.

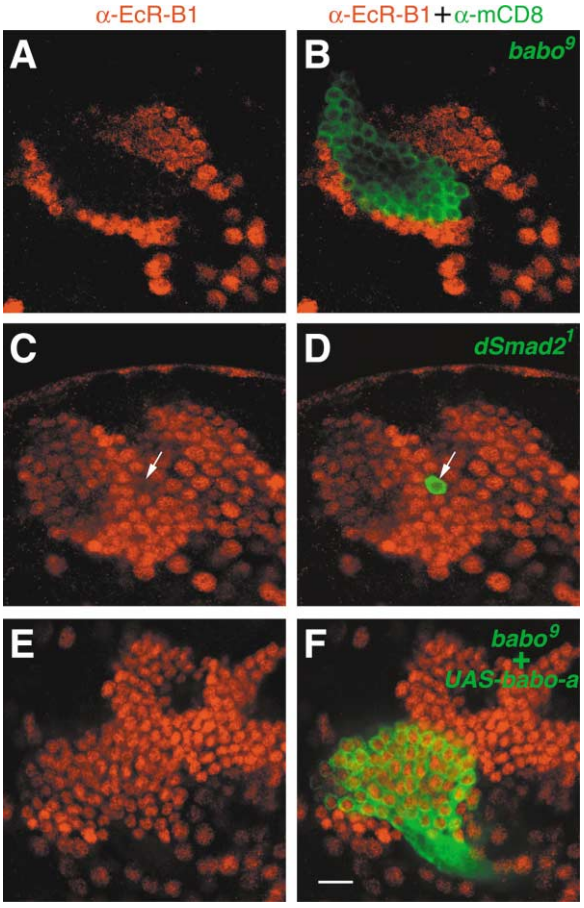

Figure 4. High-Level Expression of EcR-B1 Depends on Normal Babo/dSmad2 Activity in MB γ Neurons

Single-section confocal images of the MB cell body regions in late third instar larval brains. The brains containing mCD8-GFP-labeled MARCM clones (green) were immunostained for EcR-B1 expression (red). EcR-B1 could not be detected in either the *babo* mutant Nb clone (green in [B]) or the single-cell clone of *dSmad2* mutant γ neuron (green in [D]). Note that EcR-B1 expression was recovered in the *babo* mutant Nb clone that ectopically expressed a wild-type *babo* cDNA (green in [F]; compared with [E]). The scale bar equals 10 microns.

Genotype: (A and B) *hs-FLP/X;FRTG13,l(2R)MB224,UAS-mCD8-GFP,GAL4-201Y/FRTG13,tubP-GAL80*; (C and D) *FRT19A,l(X)MB388,UAS-mCD8-GFP/FRT19A,tubP-GAL80,hs-FLP;GAL4-201Y/+*; (E and F) *hs-FLP/UAS-babo-a;FRTG13,l(2R)MB224,UAS-mCD8-GFP,GAL4-201Y/FRTG13,tubP-GAL80*.

Restoring EcR-B1 Expression Significantly Rescues the *babo*$^{-/-}$ Remodeling Defects

Prompted by the identification of the EcR-B1 as one potential dSmad2 target gene, we reasoned that restoring EcR-B1 expression in *babo/dSmad2* mutant γ neurons might rescue their remodeling defects. To determine whether ectopic expression of EcR-B1 could rescue neuronal remodeling defects in *babo* mutant neurons, we drove expression of various EcR isoforms specifically in mutant clones and then checked dendritic elaboration and axon projection patterns of mutant neurons at the adult stage. GAL4-201Y selectively labels all γ neurons and a small subset of α/β neurons in the MBs (Yang et al., 1995). Therefore, GAL4-201Y-labeled Nb clones normally contain one weak dorsal axon bundle (the core α lobe), one weak medial bundle (the core β lobe), and one strong medial (the γ lobe) axon bundle (Figure 5A). In contrast, *babo* mutant Nb clones lack the prominent γ lobe and, instead, possess the retained larval dorsal/ventral lobes in addition to the weak core α/β lobes (data not shown; similar to Figure 5B). Interestingly, the MB γ lobe reappears in 100% of the *babo* mutant Nb clones after coexpression of the EcR-B1 with mCD8-GFP in MARCM clones (Figure 5C; n = 40), while no γ lobe is detected when the EcR-A isoform was coexpressed with mCD8GFP (Figure 5B; n = 20). Since formation of the MB γ lobe depends on normal neuronal remodeling, these observations demonstrate that restoring EcR-B1 expression alone significantly and specifically rescues *babo* loss-of-function phenotypes during remodeling of MB neurons. However, variable numbers of larval-specific dorsal branches, which are positive for GAL4-201Y, but not bundled with the core α lobe, remain in almost all the γ lobe-rescued Nb clones (Figure 5C, compared with Figure 5A), indicating that ectopic expression of EcR-B1 only partially rescues the *babo*$^{-/-}$ remodeling defects. In addition, we notice subtle neuronal remodeling after ectopic expression of EcR-B2 in *babo*$^{-/-}$ Nb clones, as evidenced by the presence of very faint γ lobes and fewer axon fibers projecting dorsally then extending medially (Figure 5D, compared with Figure 5B; n = 20).

To examine rescue of *babo* mutant neurons with single-cell resolution, we subsequently analyzed isolated single-cell clones of *babo* mutant γ neurons that simultaneously expressed the mCD8-GFP and one specific EcR isoform after loss of the GAL80 repressor. Consistent with previous findings, we observed persistence of larval dendrites and axonal branches in all the single-cell

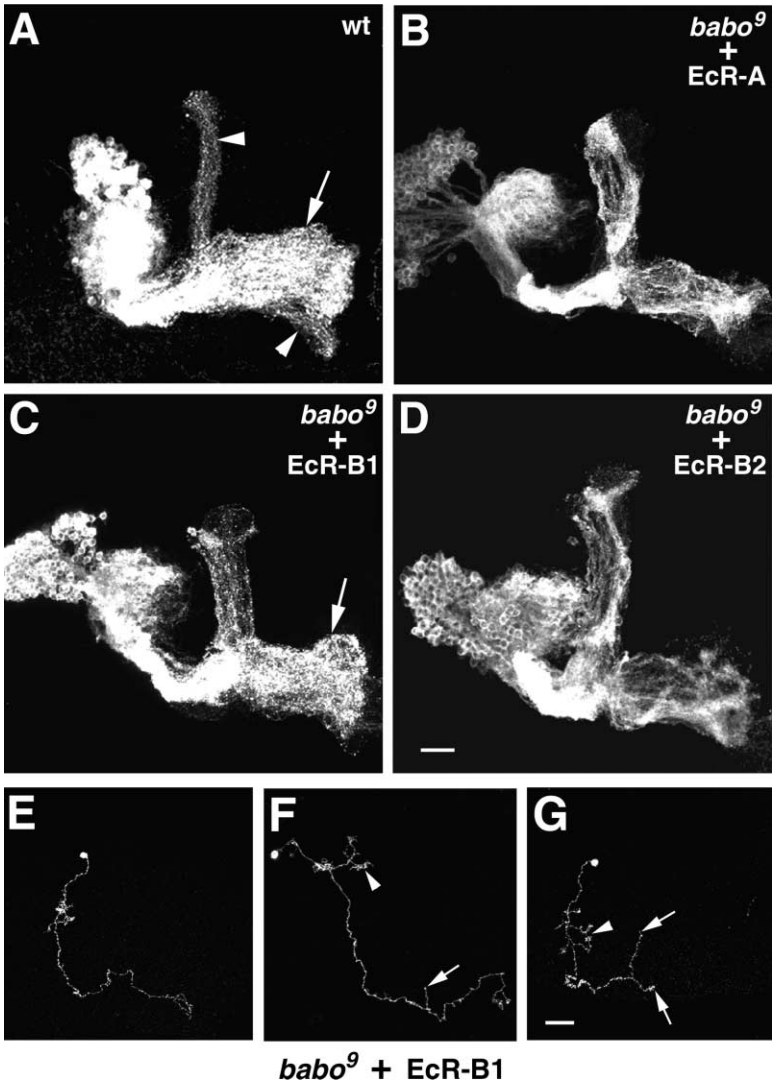

Figure 5. Ectopic Expression of Various EcR Isoforms Differentially Rescues *babo*$^{-/-}$ Neuronal Remodeling Defects

(A) When a wild-type MB Nb clone is labeled using GAL4-201Y, we observe three axon bundles at the adult stage: the big, dense γ lobe (arrow) plus the weak core α and β lobes (arrowheads).

(B–D) *babo* mutant Nb clones expressed EcR-A (B), EcR-B1 (C), or EcR-B2 (D).

(E–G) EcR-B1-rescued single-cell clones of *babo* mutant γ neurons undergo neuronal remodeling to variable extents. EcR-B1 was expressed in single-cell clones of *babo* mutant γ neurons. Truncated dorsal and medial branches (arrows in [F] and [G]) are likely derived from incomplete pruning of larval-specific axonal branches; both larval-type and adult-type dendrites (arrowheads in [F] and [G], respectively) are observed.

Genotype: (A) *hs-FLP/X ; FRTG13,UAS-mCD8-GFP,GAL4-201Y/FRTG13,tubP-GAL80*; (B) *hs-FLP/X;FRTG13,l(2R)MB224,UAS-mCD8-GFP,GAL4-201Y/FRTG13,tubP-GAL80;UAS-EcR-A/+*; (C) *hs-FLP/X;FRTG13,l(2R)MB224,UAS-mCD8-GFP,GAL4-201Y/FRTG13,tubP-GAL80;UAS-EcR-B1/+*; (D) *hs-FLP/X;FRTG13,l(2R)MB224,UAS-mCD8-GFP,GAL4-201Y/FRTG13,tubP-GAL80;UAS-EcR-B2/+*; (E–G) *hs-FLP/X;FRTG13,l(2R)MB224,UAS-mCD8-GFP,GAL4-201Y/FRTG13,tubP-GAL80;UAS-EcR-B1/+*.

clones of *babo* mutant γ neurons after ectopic expression of EcR-A or EcR-B2 (data not shown; n = 50). In contrast, variable degrees of remodeling are observed in the single-cell clones of *babo* mutant γ neurons that express EcR-B1 prior to and through metamorphosis (n = 100). Evidence for axonal remodeling exists in about 50% of mutant single-cell clones, but only about 25% of *babo*$^{-/-}$ γ neurons completely lose larval-specific branches and fully extend their adult processes (Figure 5E). In the other 25% of mutant neurons, we observe partial retraction of larval-specific axonal branches or truncation of the reextended adult processes (Figures 5F and 5G). Taken together, these results demonstrate that restoring EcR-B1 partially but significantly rescues remodeling defects in *babo* mutant neurons, supporting the notion that Babo activates EcR-B1 expression in the process of capacitating MB neuronal remodeling.

EcR-B1 Expression Is Upregulated through Two Mutually Redundant TGF-β Type II Receptors

TGF-β signaling occurs when ligand binding induces formation of heteromeric complexes between type I and II receptors. Subsequent to complex formation the type I receptor is activated by phosphorylation from the constitutively active type II receptor (Wrana et al., 1994). In *Drosophila*, there are two type II receptors encoded by the genes *punt* and *wishful thinking (wit)*. Prior molecular genetic studies have indicated that these receptors mediate distinct developmental processes (Chen et al., 1998; Aberle et al., 2002; Marques et al. 2002). To determine which type II receptor is required for activation of Babo in the remodeling process, we generated MARCM clones that were homozygous for representative *punt* or *wit* mutations. To our surprise, none of the *punt* or *wit* homozygous mutant clones exhibited any visible defects in the MB remodeling (data not shown). Thus, either these receptors are not required for remodeling, or they are redundant. To examine this issue further, we generated *wit* homozygous mutant clones in *punt*^{ts} mutant background (Simin et al., 1998). At a permissive temperature (16°C), we observe normal EcR-B1 expression in homozygous *wit* MB Nb clones at the wandering larval stage (Figures 6A and 6B). In contrast, EcR-B1 expression is selectively suppressed in *wit* mutant

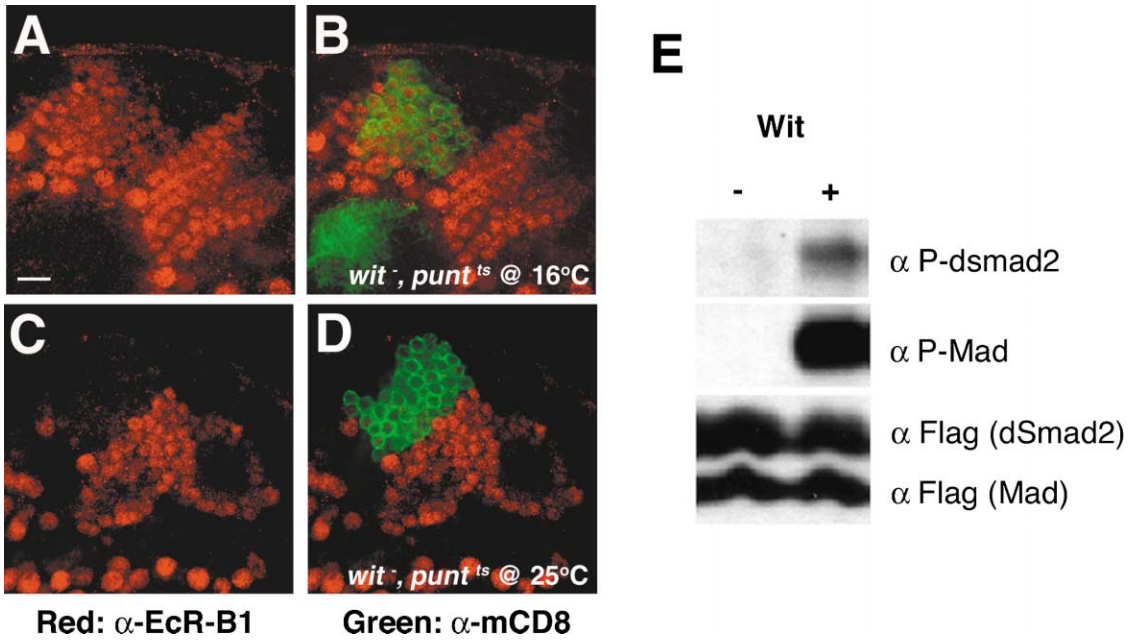

Figure 6. Punt and Wit Are Redundantly Involved in Babo-Mediated Activation of EcR-B1 Expression

(A–D) Single-section confocal images of the MB cell body regions in late third instar larval brains. The *punt*^{ts} brains containing mCD8-GFP-labeled *wit*$^{-}$ clones (green) were immunostained for EcR-B1 expression (red). Note that no EcR-B1 expression is detected in the clone (green in [D]) that has developed at 25°C. The scale bar equals 10 μm. Genotype: *hs-FLP,UAS-mCD8-GFP/X;GAL4-201Y/+;wit[G15],FRT2A,punt[135-22(ts)]/GAL80,FRT2A,punt[Δ61]*.

(E) Wit overexpression in S2 cells stimulates phosphorylation of both Mad and dSamd2. Cells were cotransfected with Mad-flag and dSmad2-flag plus or minus Wit. After 3 days of expression, extracts were prepared and analyzed for total Mad and dSmad2 protein (bottom) on Western blots using anti-flag antibody and for phosphorylated forms of these proteins using anti-P-Mad or anti-P-Smad2 antibody (top).

clones if *punt*^{ts} larvae have developed continuously at the restrictive temperature (25°C) after clone induction (Figures 6C and 6D). Therefore, Punt and Wit are redundantly involved in activating Babo-dependent EcR-B1 expression.

Taking advantage of such a temperature-sensitive background, we tried to determine when TGF-β signaling is required during induction of EcR-B1 expression. We generated homozygous *wit*$^{-}$ clones in temperature-sensitive *punt* mutant organisms that were then incubated at various temperatures during subsequent developmental stages. We noticed that development was much delayed if larvae remained at 25°C, but these larvae could grow into mature larvae with normal EcR-B1 expression if they were transferred to 16°C prior to the third instar stage. However, *wit* mutant MB Nb clones (n = 12) exhibited no EcR-B1 expression if mosaic organisms were transferred to the restricted temperature at the beginning of the third instar larval stage. In contrast, 50% of the mutant clones (n = 8) acquired normal EcR-B1 expression if they were transferred around the mid-third instar stage. Interestingly, no clone contained a mixture of EcR-B1-positive and EcR-B1-negative γ neurons. These phenomena suggest that TGF-β signaling modulates EcR-B1 expression roughly around the mid-third instar stage.

Since Wit has been previously demonstrated to function in a BMP signaling pathway (Marques et al. 2002), we sought biochemical evidence to support a possible role in TGF-β/Activin signaling as well. To examine this issue, we took advantage of the fact that overexpression of type II receptors can activate signaling pathways in a ligand independent manner (Feng and Derynck 1996). S2 cells, which do not express *wit* (data not shown), were transfected with both Mad-flag and dSmad2-flag plus or minus Wit. These cells were then examined for total Mad or dSmad2 expression by Western blots using anti-flag antibody and for phosphorylation of Mad (P-Mad) or dSmad2 (P-dSmad2) using antibodies specific for the phosphorylated forms of these proteins. As shown in Figure 6E, overexpression of Wit leads to phosphorylation of both Mad and dSamd2. This observation, together with the genetic data, supports the notion that Punt and Wit play redundant roles in remodeling neurons.

dActivin, Like Babo, Is Required for Both Optic Lobe Development and EcR-B1 Expression in Larval Brains

We also wished to identify possible ligands that participate in the remodeling process. Seven TGF-β type ligands are present in the *Drosophila* genome. Three of these, *dpp, scw,* and *gbb*, are clearly of the BMP family (Newfeld et al. 1999). The remaining, *maverick (mav)* (Nguyen et al., 2000), *myoglianin (myo), dActivin (dAct)* (Kutty et al., 1998), and *activin-like-protein (alp)*, have not been assigned either genetically or biochemically to a particular family or signaling pathway. Phylogenetic considerations place dAct clearly within the Activin subfamily (Newfeld et al. 1999), while Myo is most similar to BMP-11 and GDF-8 (Lo and Frasch, 1999), and Mav and Alp are equidistant from both the BMP and TGF-β/

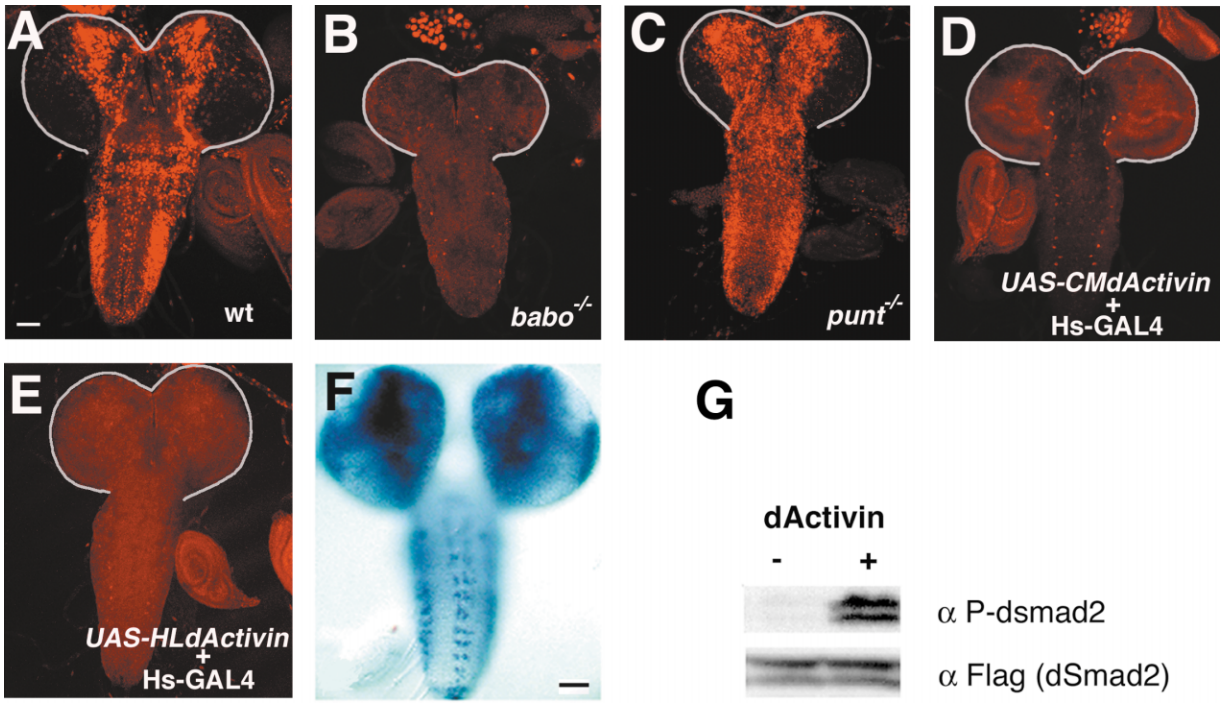

Figure 7. dActivin Is Required for Normal EcR-B1 Expression in Late Third Instar Larval Brains

(A–E) Various wandering larvae were dissected and examined for EcR-B1 expression (red) in the CNS. The wild-type EcR-B1 expression pattern is maintained in the small *punt*⁻ CNS (compare [C] with [A]). In contrast, EcR-B1 expression is largely missing in the *babo*⁻ CNS (compare [B] with [A] and [C]) or after transient expression of cleavage-defective *dActivin* or hairpin-loop *dActivin* between 1–2 days before dissection (compare [D] and [E] with [A] and [C]). The brains are outlined by gray curves. The scale bar equals 40 μm. Genotype: (A) *w[1118]*; (B) *babo[k16912]/babo[52]*; (C) *wit[G15],FRT2A,punt[135-22(ts)]/GAL80,FRT2A,punt[Δ61]*; (D) *UAS-CMdActivin/Hs-GAL4*; (E) *UAS-HLdActivin/Hs-GAL4*.

(F) dActivin expression in the early third instar larval CNS is revealed by in situ hybridization.

(G) Addition of dActivin to S2 cells transfected with dSmad2 results in phosphorylation of dSmad2. Western blots were incubated with the indicated antibodies.

Activin subgroups. Therefore, we decided to examine possible involvement of dAct in the Babo signaling.

First, in situ hybridization revealed that dAct is widely expressed in larval brains (Figure 7F; data not shown for negative staining with sense probes). Second, when conditioned media from cells expressing dAct was added to S2 cells transfected with dSmad2, we found that this ligand is able to stimulate phosphorylation of dSmad2 (Figure 7G), while the prototypical BMP ligand Dpp is not (data not shown). Third, we tried to knock out dAct activity using two independent approaches and found that dAct, like Babo, is essential for both optic lobe development and EcR-B1 expression in larval brains. Since *dAct* mutations are currently unavailable, we sought to produce a partial loss-of-function condition by overexpression of a dominant-negative form of the protein or RNAi (Piccin et al., 2001). All TGF-β type ligands that have been examined dimerize and are processed prior to secretion. Previous studies have shown that overexpression of a cleavage-defective form of a particular ligand can interfere with processing and secretion of endogenous ligand (Osada and Wright 1999). Therefore, we overexpressed a cleavage defective form of dAct (CMdAct) using either a general GAL4 driver (tubP-GAL4) or an MB-specific driver (GAL4-OK107). We observe that CNS development is retarded only when the CMdAct is ubiquitously expressed and not when it is expressed in MBs. This suggests that dAct does not function within MBs in an autocrine-like fashion. Poor development of the optic lobes is apparent in the tubP-GAL4>CMdAct larval brains, similar to that observed in *babo* and *punt* mutant larvae (Figures 7B and 7C, and data not shown). More importantly, EcR-B1 expression is largely absent in γ neurons of animals that ubiquitously express CMdAct, similar to what is observed in *babo* mutants (Figure 7B). Hs-GAL4-mediated transient expression of CMdAct around the mid-third instar stage also blocks both optic lobe development and EcR-B1 expression (53%, n = 34; Figure 7D). Consistent results are obtained after induction of RNAi using a hairpin-loop *dAct* construct (UAS-HLdAct). For instance, we detect no EcR-B1 expression in 65% of the late third instar larval brains (n = 40) that were heat shocked to express UAS-HLdAct transiently around the mid-third instar stage (Figure 7E). Again, absence of EcR-B1 expression is tightly associated with poor optic lobe development. Similar treatments yield no detectable phenotypes when UAS-CMdAct/UAS-HLdAct is absent or replaced with other UAS-transgenes, such as UAS-mCD8-GFP and UAS-antisense dActivin (data not shown). In addition, *punt* mutants, despite having small brains, continue to show EcR-B1 expression (Figure 7C).

Taken together, these results suggest that dAct, like Babo and dSmad2, is indispensable for EcR-B1 expression in the CNS of wandering larvae.

Discussion

Roles of TGF-β Signaling in Neuronal Plasticity

From forward genetic mosaic screens we found that the Babo TGF-β/Activin type I receptor and a well-known TGF-β/Activin receptor downstream effector, dSmad2, are both cell autonomously required for remodeling of MB neurons during metamorphosis, providing definitive evidence for involvement of TGF-β/Activin signaling in neuronal plasticity. No evidence exists for any cell fate change in *babo* mutant MB neurons. For instance, expression of multiple cell type-specific markers remains normal (data not shown), and mutant γ neurons, unlike wild-type α′/β′ neurons, consistently acquire mature dendritic morphological features before metamorphosis (Figure 1). In addition, MB γ neurons that are born at various stages all commit to expressing EcR-B1 in response to TGF-β signaling at the same time and after they all develop into morphologically mature neurons. Therefore, TGF-β signaling probably plays a direct role in programming neuronal plasticity and is not required for cell specification.

TGF-β signaling is implicated in regulating neuronal plasticity in diverse organisms (reviewed in Ebendal et al., 1998; Patterson and Padgett, 2000). For instance, environmental cues regulate synthesis of a TGF-β-related ligand (DAF-7) in a pair of chemosensory neurons in *C. elegans* to direct entry into and exit from an alternative third larval stage called the dauer larva (Ren et al., 1996). Dauer formation involves arrest of all postembryonic cell divisions and remodeling of various tissues throughout the body (reviewed in Riddle and Albert, 1997). Given that the DAF-7 TGF-β ligand is primarily sensed by neurons expressing appropriate TGF-β receptors and Smads, it is likely that changes in TGF-β activities directly mediate neuronal remodeling and in turn orchestrate diverse dauer entry/exit responses outside the nervous system (Inoue and Thomas, 2000). However, it remains to be elucidated whether and how TGF-β signaling regulates neuronal projections and connections in individual remodeling neurons during the entry into and exit from the dauer stage.

In *Drosophila*, recent data suggests that a BMP signaling pathway controls synaptic growth and function at the neuromuscular junction (NMJ). Whether this pathway also contributes to activity-dependent remodeling at the NMJ remains to be determined. It is interesting to note, however, that in this pathway Wit acts as a BMP receptor, and it can not be substituted for by Punt (Marques et al. 2002). In contrast, the activin pathway described here appears to be able to utilize either Punt or Wit for signaling. This may reflect selectivity in the binding of some ligands to one receptor, but not the other. Additional studies will be required to resolve this issue. Since many components of several different TGF-β signaling pathways show pronounced expression in different parts of the developing and postnatal rodent brain (Ebendal et al., 1998), our demonstration that TGF-β/Activin signaling cell-autonomously controls plasticity of MB neurons may provide novel insights into how neuroplasticity is dynamically regulated in higher organisms.

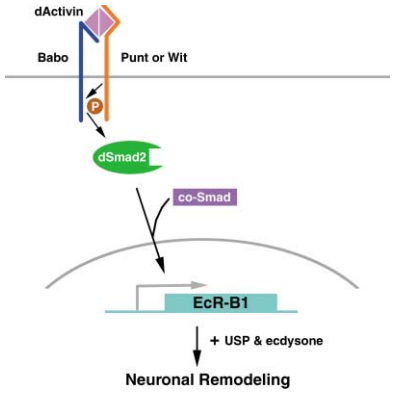

Figure 8. A Schematic Model for Babo-/dSmad2-Mediated Neuronal Remodeling

TGF-β signaling involves ligand (dActivin)-dependent binding of TGF-β type I receptors (Babo) with TGF-β type II receptors (Punt/Wit) followed by phosphorylation and activation of the type I receptors. In MB γ neurons, activated Babo in turn phosphorylates the dSmad2 proteins. Phosphorylated dSmad2 proteins, probably in complexes with co-Smads, then shuttle into the nucleus, eventually leading to high-level expression of the EcR-B1 isoform. Around puparium formation, binding of ecdysone to the EcR-B1/USP heterodimeric receptors initiates neuronal remodeling via transcriptional activation of unidentified target genes.

Activation of EcR-B1 Expression by TGF-β Signaling

Changes in gene expression are believed to mediate most TGF-β-dependent biological processes (Massague and Chen, 2000). Our observation that restoration of EcR-B1 expression significantly rescued remodeling defects in *babo* mutant neurons supports the model that the Babo/dSmad2-mediated TGF-β signaling mediates neuronal remodeling via upregulation of the EcR-B1 expression (Figure 8). Interestingly, ecdysone has also recently been implicated in regulating synaptic efficacy at the *Drosophila* NMJ (Li and Cooper, 2001), as has BMP signaling (Aberle et al., 2002; Marques et al., 2002). However, as yet no connection between TGF-β signaling and the ecdysone pathway has been established in this system. In *C. elegans*, the DAF-7 TGF-β ligand as well as the DAF-12 nuclear hormone receptor are involved in dauer formation (Antebi et al., 2000). In response to hormonal signals, DAF-12 and EcR coordinate changes in diverse tissues during dauer formation and metamorphosis, respectively. Therefore it might be a common theme that TGF-β signaling patterns tissue-specific responses to steroid hormones in diverse organisms by regulating expression and/or activities of specific steroid hormone receptors.

Several lines of evidence support the model that patterned EcR-B1 expression in the late third instar larval CNS is likely established as a consequence of stage-regulated, cell type-specific responses to TGF-β signaling. First, dActivin is broadly expressed in the CNS, while expression of EcR-B1 is selectively restricted. Second, despite the persistent presence of dActivin expression

during all developmental stages and the fact that γ neurons are born at different times, programming of EcR-B1 expression in γ neurons does not occur until the mid-third instar stage. Third, ubiquitous expression of activated Babo fails to activate EcR-B1 expression ectopically (our unpublished data). Determining how TGF-β signaling induces such stage-specific, cell type-dependent responses will provide mechanistic cues for how EcR-B1 is differentially expressed to pattern metamorphosis of the CNS. Possible models might include differential expression of a dSmad2 cofactor or the requirement for a second signal that cooperates with the dActivin signal. Lastly, it will be important to determine how dActivin reaches its target MB neurons. As has been recently suggested for BMP signaling at the NMJ (Aberle et al. 2002; Marques et al. 2002), this might involve retrograde signaling from the MB synapse or it may occur via a juxtacrine mechanism from nearby cells.

Gaps between Nuclear Signaling and Cytoskeleton Dynamics

No direct connection has been shown between TGF-β signaling and regulation of cytoskeleton dynamics. Consistent with vital roles of TGF-β pathways in regulating gene expression, our results suggest that Babo/dSmad2 signaling might simply lead to activation of EcR-B1 expression to capacitate MB neuronal remodeling during metamorphosis. Although this study provides novel insights into how differential expression of EcR isoforms is achieved, the challenge now is how ecdysone-induced transcriptional hierarchies mediate complex cytoskeletal changes in remodeling neurons. Identifying mutations that block various aspects of the MB neuronal remodeling in mosaic organisms will continue to shed new light on the molecular mechanisms underlying neuronal plasticity.

Experimental Procedures

Fly Strains

Creation of *babo* MARCM clones involves (1) *hs-FLP;FRTG13,tubP-GAL80/CyO*, (2) *UAS-mCD8-GFP,hs-FLP;FRTG13,tubP-GAL80/CyO;GAL4-OK107*, (3) *FRTG13,l(2R)MB224,UAS-mCD8-GFP,GAL4-201Y/CyO*, (4) *FRTG13,babo[Fd4]/CyO*, and (5) *FRTG13,babo[52]/CyO*. Creation of *dSmad2* MARCM clones involves (6) *FRT19A,tubP-GAL80,hs-FLP;GAL4-201Y*, and (7) *FRT19A,l(X)MB388,UAS-mCD8-GFP*. (8) *FRTG13,UAS-mCD8-GFP,GAL4-201Y* was used for creating wild-type MARCM clones. Creation of *punt* or *wit* MARCM clones involves (9) FRT82B,punt[Δ61]/TM6B, (10) *FRT82B,punt[135-22(ts)]/TM6B*, (11) *wit[G15],FRT2A/TM6B*, (12) *wit[G15],FRT2A,punt[135-22(ts)]/TM6B*, and (13) *tubP-GAL80,FRT2A,punt[Δ61]/TM6B*. Ectopic expression of various transgenes in MARCM clones involves (14) *UAS-babo-a*, (15) *UAS-dSmad2*, (16) *UAS-EcR-A* (Lee et al., 2000a), (17) *UAS-EcR-B1* (Lee et al., 2000a), (18) *UAS-EcR-B2* (Lee et al., 2000a), (19) UAS-activated babo (Brummel et al., 1999), (20) UAS-CMdActivin, (21) UAS-HLdActivin, (22) *tubP-GAL4* (Lee and Luo, 1999), (23) *elav-GAL4* (Luo et al., 1994), (24) *GAL4-OK107* (Connolly et al., 1996), and (25) *Hs-GAL4* (for transient expression of UAS-CMdActivin and UAS-HLdActivin).

Other fly stocks collected for this study include *ec,cv,ct,t/C(1)DX* (BL-1163), *y,ct,ras,f* (BL-4362), *Df(2R)H3E1* (BL-201), *Df(2R)Np1* (BL-6091), *Df(2R)Np4* (BL-5423), *Df(2R)G75* (BL-6090), *Df(1)RA2* (BL-950), *Df(1)GE202* (BL-1879), *Df(1)C128* (BL-2984), *Df(1)Desi-S3* (a gift from D. Andrew), *Df(1)hl-a* (a gift from N. Perrimon), *Dp(1;2)Sn$^+$72d* (BL-1879), *flz^1/CyO* (BL-3271), *lin^2/CyO* (BL-3099), *l(2)44Fj^1/CyO* (BL-5507), *l(2)44Fc^3/CyO* (BL-5502), *babo^{32}/CyO* (BL-5399), and *babo^{k16912}/CyO* (BL-11207).

MARCM-Based Genetic Screens

Our ongoing genetic mosaic screens have been reported before (Lee et al., 2000a; Wang et al., 2002). Briefly, MARCM clones of MB neurons, which are homozygous for EMS-mutagenized X or 2R chromosome arms, were created and screened for abnormal neurogenesis or neuronal morphogenesis. Mutant chromosomes with interesting phenotypes were then recovered for future analysis.

Mapping by Recombination and Complementation

After learning that the *l(2R)MB224* line was homozygous lethal, we tried to map the lethal mutations(s) using the 2R deficiency kit from the Bloomington Stock Center. Only *Df(2R)H3E1* failed to complement with *l(2R)MB224*, localizing one lethal mutation to the 44D–44F region. Further complementation assays using *Df(2R)Np1*, *Df(2R)G75*, and *Df(2R)Np4* allowed us to map the lethal mutation into a region that only contains two lethal complementation groups (Figure 2A) (Dockendorff et al., 2000). We later found that *l(2R)MB224* failed to complement with several known *babo* mutations, confirming that *l(2R)MB224* carries a lethal mutation in the *babo* gene.

Regarding *l(X)MB388*, homologous recombination was first induced between the *FRT19A,UAS-mCD8-GFP* mutant chromosome and an X chromosome carrying multiple visible mutations. Hemizygous male progeny were collected and analyzed for viable recombination patterns. Based on recombination patterns, *l(X)MB388* mutation(s) should be proximal to *ct* (7B). Moreover, it appeared to be linked with *ct*, given that recombination between the *l(X)MB388* mutation(s) and *ct* occurred at about 25% of the recombination frequency between *ct* and *cv* (5B). Then, using *Dp(1;2)Sn$^+$72d* that carries a translocated 7A–8A genomic fragment, we rescued *l(X)MB388* and subsequently localized one lethal mutation to the 7D10–7D12 region based on complementation tests with several deficiency lines (Figure 3A) (Henderson and Andrew, 1998).

PCR Amplification and Sequence Analysis of the *dSmad2^1* and *babo^{Fd4}* Allele

For *dSmad2*, three pairs of primers, (AGTTCATCCTGGTAGTTGAC/CATGTGTGTGCGTGAGCG, GATTACCCATATACACACGCT/ATGCTGCTGCCCACACTAAG, and CTCGTCGTCGTCGTCGTCATC/ACTACAAAGCCGAACAAAAGCAC), were used to PCR amplify the entire *dSmad2* genomic region from the wild-type *FRT19A,UAS-mCD8-GFP* chromosome and the *l(X)MB388* mutant chromosome. PCR products from multiple independent PCR reactions were subcloned into the pBS and then cycle-sequenced by Qiagen.

For the *babo^{Fd4}* allele, genomic DNA for exons 5–8 were amplified by PCR and sequenced. *babo^{Fd4}* was found to exhibit a deletion/insertion of a few nucleotides at the exon/intron 7 boundary (see alignment sequence). Consequently, the mutant gene most likely produces a truncated receptor that lacks the last exon (60 amino acids). Since most of the protein is still made, *babo^{Fd4}* may be an antimorphic allele.

```
Wild-type: AAG AAG/GTG AGT CTT TCA AGG AAC AAA ACG AAT GTG
Wt protein: K   K / intron 7  –  –  –  –  –  –  –  –
Fd4 mutant: AAG AAG AAG GTC TTT CAA GGA ACA AAA CGA ATG TGG
Fd4 protein: K  K  K  V  F  Q  G  T  K  R  M  W
Wild-type: GAC TCG TGT CAT AAT TTC ATA ATT TCT CTA AAG/GTG
Wt protein: –  –  –  –  –  –  –  –  –  intron7 / V
Fd4 mutant: ACT CGT GTC ATA ATT TCA TAA
Fd4 protein: T  R  V  I  I  S  *
```

Construction of *UAS-babo-a*, *UAS-dSmad2*, *UAS-CMdActivin*, and *UAS-HLdActivin*

For pUAST-babo-a, a 3.3 kb EcoRI fragment containing the entire *babo-a* open reading frame was filled in with Klenow and blunt end cloned into a filled in BglII site of pUAST. For pUAST-dSmad2, a 3.1 kb SalI (blunted)-NotI fragment of *dSmad2* was cloned into the StuI-NotI site of pAcpA. From this vector, a BamHI (blunted)-NotI fragment was cloned into the EcoRI (blunted)-NotI sites of pUAST. To generate the cleavage mutant of dActivin (CMdActivin), arginine residues 563–565 immediately upstream of the putative processing site were converted to alanine using the Stratagene quick change system. Subsequently, a filled in Eco R1-Not1 fragment was cloned into the BglI site of pUAST. The hairpin-loop dActivin (HLdActivin) construct was created by piecing together an 1.3 kb dActivin frag-

ment (Xho to HindIII) with another fragment already containing GFP and an inverted 1.3 kb dActivin in the pUAST vector.

Phenotypic Analysis and Rescue of MARCM Clones

MARCM clones of MB neurons were generated in NHL and examined later, as described previously (Lee et al., 2000b). MARCM clones were labeled using the rat anti-mCD8 mAb (1:100, Caltag), and EcR-B1 was detected by the AD4.4 mAb (1:20; Talbot et al., 1993). Rescue of MARCM clones involves GAL4-dependent coexpression of the mCD8-GFP and various UAS-transgenes in clones of GAL80-minus neurons.

Phosphorylation of dSmad2 in Cultured Cells

For more efficient expression in tissue culture cells, the signal sequence of dActivin was replaced by the corresponding sequence of TKV2 in pAcpA (pBR322 derivative containing an Actin5C promoter and polyA signal). 4×10^7 cells were either transfected with 20 μg of this construct or with pAcpA (no insert) as a control, as previously described (Ross et al. 2001). In parallel, 4×10^7 cells were cotransfected with 3 μg of pAcpA-Flag-Mad and pAcpA-Flag-dSmad2. After 4 days, the supernatants of the control (pAcpA) and the dActivin-expressing cells were collected and individually incubated with 1×10^7 cells that were transfected with the Mad and dSmad2 constructs. After 4 hr, the cells were precipitated and lyzed in 120 μl of cell lysis buffer (50 mM Tris-Cl [pH 7.4], 150mM NaCl, 1% Triton X-100). After centrifugation, 9 μl of the samples were mixed with 3 μl of 4$\times$ DNA loading dye and analyzed by Western blotting.

For Wit signaling assays, 2×10^7 cells were cotransfected with 1 μg of pAcpA-Wit, 3 μg of pAcpA-Flag-Mad, and pAcpA-Flag-dSmad2. As a control, 1 μg of pAcpA (no insert) was cotransfected with pAcpA-Flag-Mad and pAcpA-Flag-dSmad. After 3 days, the cells were collected by centrifugation, lyzed, and analyzed as indicated above.

In Situ Hybridization

In situ hybridization was carried out as described in Brummel et al., 1999.

Acknowledgments

We thank D. Andrew for the *Df(1)Desi-S3*, N. Perrimon for the *Df(1)hl-a*, S. Robinow for *UAS-EcR* flies, the Bloomington Stock Center for other mutant flies, C. Thummel for anti-EcR antibodies, and P. ten Dike for anti P-Mad and anti P-Smad2 antibodies. We thank D. Montell, G. Robinson, and members of the Lee lab, especially C.T. Zugates, for comments on the manuscript. This work was supported by National Institutes of Health Grant NS42049 to T.L. T.L. is a Klingenstein fellow and a Sloan fellow, and M.B.O. is an associate investigator with the Howard Hughes Medical Institute.

Received: June 19, 2002
Revised: January 2, 2003

References

Aberle, H., Haghighi, A.P., Fetter, R.D., McCabe, B.D., Magalhaes, T.R., and Goodman, C.S. (2002). wishful thinking encodes a BMP type II receptor that regulates synaptic growth in *Drosophila*. Neuron *33*, 545–558.

Antebi, A., Yeh, W.H., Tait, D., Hedgecock, E.M., and Riddle, D.L. (2000). daf-12 encodes a nuclear receptor that regulates the dauer diapause and developmental age in *C. elegans*. Genes Dev. *14*, 1512–1527.

Bender, M., Imam, F.B., Talbot, W.S., Ganetzky, B., and Hogness, D.S. (1997). *Drosophila* ecdysone receptor mutations reveal functional differences among receptor isoforms. Cell *91*, 777–788.

Brummel, T., Abdollah, S., Haerry, T.E., Shimell, M.J., Merriam, J., Raftery, L., Wrana, J.L., and O'Connor, M.B. (1999). The *Drosophila* activin receptor baboon signals through dSmad2 and controls cell proliferation but not patterning during larval development. Genes Dev. *13*, 98–111.

Chen, Y., Riese, M.J., Killinger, M.A., and Hoffmann, F.M. (1998). A genetic screen for modifiers of *Drosophila* decapentaplegic signaling identifies mutations in punt, Mothers against dpp and the BMP-7 homologue, 60A. Development *125*, 1759–1768.

Connolly, J.B., Roberts, I.J., Armstrong, J.D., Kaiser, K., Forte, M., Tully, T., and O'Kane, C.J. (1996). Associative learning disrupted by impaired Gs signaling in *Drosophila* mushroom bodies. Science *274*, 2104–2107.

Das, P., Inoue, H., Baker, J.C., Beppu, H., Kawabata, M., Harland, R.M., Miyazono, K., and Padgett, R.W. (1999). *Drosophila* dSmad2 and Atr-I transmit activin/TGFbeta signals. Genes Cells *4*, 123–134.

de Belle, J.S., and Heisenberg, M. (1994). Associative odor learning in *Drosophila* abolished by chemical ablation of mushroom bodies. Science *263*, 692–695.

Derynck, R., Zhang, Y., and Feng, X.H. (1998). Smads: transcriptional activators of TGF-beta responses. Cell *95*, 737–740.

Dockendorff, T.C., Robertson, S.E., Faulkner, D.L., and Jongens, T.A. (2000). Genetic characterization of the 44D–45B region of the *Drosophila melanogaster* genome based on an F2 lethal screen. Mol. Gen. Genet. *263*, 137–143.

Ebendal, T., Bengtsson, H., and Soderstrom, S. (1998). Bone morphogenetic proteins and their receptors: potential functions in the brain. J. Neurosci. Res. *51*, 139–146.

Feng, X.-H., and Derynck, S. (1996). Ligand-independent activation of transforming growth factor (TGF) β signaling pathways by heteromeric cytoplasmic domains of TGF-β receptors. J. Biol. Chem. *271*, 13123–13129.

Heldin, C.H., Miyazono, K., and ten Dijke, P. (1997). TGF-beta signalling from cell membrane to nucleus through SMAD proteins. Nature *390*, 465–471.

Henderson, K.D., and Andrew, D.J. (1998). Identification of a novel *Drosophila* SMAD on the X chromosome. Biochem. Biophys. Res. Commun. *252*, 195–201.

Hubel, D.H., Wiesel, T.N., and LeVay, S. (1977). Plasticity of ocular dominance columns in monkey striate cortex. Philos. Trans. R. Soc. Lond. B Biol. Sci. *278*, 377–409.

Inoue, T., and Thomas, J.H. (2000). Targets of TGF-beta signaling in *Caenorhabditis elegans* dauer formation. Dev. Biol. *217*, 192–204.

Iyengar, S., and Bottjer, S.W. (2002). Development of individual axon arbors in a thalamocortical circuit necessary for song learning in zebra finches. J. Neurosci. *22*, 901–911.

Konev, Au.I., Varentsova, E.R., and Khromykh, Iu.M. (1994). Cytogenetic analysis of the chromosome region containing the *Drosophila* radiosensitivity gene. II. The vitally important loci of the 44F–45C region of chromosome 2. Genetika *30*, 201–211.

Kutty, G., Kutty, R.K., Samuel, W., Duncan, T., Jaworski, C., and Wiggert, B. (1998). Identification of a new member of transforming growth factor-beta superfamily in *Drosophila*: the first invertebrate activin gene. Biochem. Biophys. Res. Commun. *246*, 644–649.

Lee, T., and Luo, L. (1999). Mosaic analysis with a repressible cell marker for studies of gene function in neuronal morphogenesis. Neuron *22*, 451–461.

Lee, T., and Luo, L. (2001). Mosaic analysis with a repressible cell marker (MARCM) for *Drosophila* neural development. Trends Neurosci. *24*, 251–254.

Lee, T., Lee, A., and Luo, L. (1999). Development of the *Drosophila* mushroom bodies: sequential generation of three distinct types of neurons from a neuroblast. Development *126*, 4065–4076.

Lee, T., Marticke, S., Sung, C., Robinow, S., and Luo, L. (2000a). Cell autonomous requirement of the USP/EcR-B ecdysone receptor for mushroom body neuronal remodeling. Neuron *28*, 807–818.

Lee, T., Winter, C., Marticke, S.S., Lee, A., and Luo, L. (2000b). Essential roles of *Drosophila* RhoA in the regulation of neuroblast proliferation and dendritic but not axonal morphogenesis. Neuron *25*, 307–316.

Levine, R.B. (1984). Changes in neuronal circuits during insect metamorphosis. J. Exp. Biol. *112*, 27–44.

Levine, R.B., Morton, D.B., and Restifo, L.L. (1995). Remodeling of the insect nervous system. Curr. Opin. Neurobiol. *5*, 28–35.

Li, H., and Cooper, R.L. (2001). Effects of the ecdysoneless mutant on synaptic efficacy and structure at the neuromuscular junction in *Drosophila* larvae during normal and prolonged development. Neuroscience *106*, 193–200.

Lo, P.C., and Frasch, M. (1999). Sequence and expression of myoglianin, a novel *Drosophila* gene of the TGF-beta superfamily. Mech. Dev. *86*, 171–175.

Luo, L., Liao, Y.J., Jan, L.Y., and Jan, Y.N. (1994). Distinct morphogenetic functions of similar small GTPases: *Drosophila* Drac1 is involved in axonal outgrowth and myoblast fusion. Genes Dev. *8*, 1787–1802.

Marques, G., Bao, H., Haerry, T.E., Shimell, M.J., Duchek, P., Zhang, B., and O'Connor, M.B. (2002). The *Drosophila* BMP type II receptor Wishful Thinking regulates neuromuscular synapse morphology and function. Neuron *33*, 529–543.

Massague, J. (1998). TGF-beta signal transduction. Annu. Rev. Biochem. *67*, 753–791.

Massague, J., and Chen, Y.G. (2000). Controlling TGF-beta signaling. Genes Dev. *14*, 627–644.

Murakami, F., Song, W.J., and Katsumaru, H. (1992). Plasticity of neuronal connections in developing brains of mammals. Neurosci. Res. *15*, 235–253.

Newfeld, S.J., Wisotzkey, R.G., and Kumar, S. (1999). Molecular evolution of a developmental pathway: phylogenetic analyses of transforming growth factor-beta family ligands, receptors and Smad signal transducers. Genetics *152*, 783–795.

Nguyen, M., Parker, L., and Arora, K. (2000). Identification of maverick, a novel member of the TGF-beta superfamily in *Drosophila*. Mech. Dev. *95*, 201–206.

O'Leary, D.D., and Koester, S.E. (1993). Development of projection neuron types, axon pathways, and patterned connections of the mammalian cortex. Neuron *10*, 991–1006.

Osada, S.I., and Wright, C.V. (1999). Xenopus nodal-related signaling is essential for mesendodermal patterning during early embryogenesis. Development *126*, 3229–3240.

Patterson, G.I., and Padgett, R.W. (2000). TGF beta-related pathways. Roles in *Caenorhabditis elegans* development. Trends Genet. *16*, 27–33.

Piccin, A., Salameh, A., Benna, C., Sandrelli, F., Mazzotta, G., Zordan, M., Rosato, E., Kyriacou, C.P., and Costa, R. (2001). Efficient and heritable functional knock-out of an adult phenotype in *Drosophila* using a GAL4-driven hairpin RNA incorporating a heterologous spacer. Nucleic Acids Res. *29*, E55–5.

Raftery, L.A., and Sutherland, D.J. (1999). TGF-beta family signal transduction in *Drosophila* development: from Mad to Smads. Dev. Biol. *210*, 251–268.

Ren, P., Lim, C.S., Johnsen, R., Albert, P.S., Pilgrim, D., and Riddle, D.L. (1996). Control of *C. elegans* larval development by neuronal expression of a TGF-beta homolog. Science *274*, 1389–1391.

Riddle, D.L., and Albert, P.S. (1997). Genetic and environmental regulation of dauer larva development. . D.L. Riddle, T. Blumenthal, B.J. Meyer, and P.J.R., eds. (Cold Spring Harbor, New York: Cold Spring Harbor Laboratory Press), pp. 739–768.

Ross, J., Shimmi, O., Vilmos, P., Petryk, A., Kim, H., Gaudenz, K., Hermanson, S., Ekker, S.C., O'Connor, M.B., and Marsh, J.L. (2001). Twisted gastrulation is a conserved extracellular BMP antagonist. Nature *410*, 479–483.

Savage-Dunn, C. (2001). Targets of TGF beta-related signaling in *Caenorhabditis elegans*. Cytokine Growth Factor Rev. *12*, 305–312.

Simin, K., Bates, E.A., Homer, M.A., and Letsou, A. (1998). Genetic analysis of *punt*, a type II Dpp receptor that functions throughout the *Drosophila melanogaster* life cycle. Genetics *148*, 801–813.

Talbot, W.S., Swyryd, E.A., and Hogness, D.S. (1993). *Drosophila* tissues with different metamorphic responses to ecdysone express different ecdysone receptor isoforms. Cell *73*, 1323–1337.

Technau, G., and Heisenberg, M. (1982). Neural reorganization during metamorphosis of the corpora pedunculata in *Drosophila melanogaster*. Nature *295*, 405–407.

Thomas, H.E., Stunnenberg, H.G., and Stewart, A.F. (1993). Heterodimerization of the *Drosophila* ecdysone receptor with retinoid X receptor and ultraspiracle. Nature *362*, 471–475.

Thummel, C.S. (1996). Files on steroids–*Drosophila* metamorphosis and the mechanisms of steroid hormone action. Trends Genet. *12*, 306–310.

Truman, J.W. (1990). Metamorphosis of the central nervous system of *Drosophila*. J. Neurobiol. *21*, 1072–1084.

Truman, J.W., Talbot, W.S., Fahrbach, S.E., and Hogness, D.S. (1994). Ecdysone receptor expression in the CNS correlates with stage-specific responses to ecdysteroids during *Drosophila* and *Manduca* development. Development *120*, 219–234.

Wang, J., Zugates, C.T., Liang, I.H., Lee, C.-H.J., and Lee, T. (2002). *Drosophila* Dscam is required for divergent segregation of sister branches and suppresses ectopic bifurcation of axons. Neuron *33*, 559–571.

Wrana, J.L., Attisano, L., Wieser, R., Ventura, F., and Massague, J. (1994). Mechanism of activation of the TGF-beta receptor. Nature *370*, 341–347.

Wu, J.W., Hu, M., Chai, J., Seoane, J., Huse, M., Li, C., Rigotti, D.J., Kyin, S., Muir, T.W., Fairman, R., et al. (2001). Crystal structure of a phosphorylated Smad2. Recognition of phosphoserine by the MH2 domain and insights on Smad function in TGF-beta signaling. Mol. Cell *8*, 1277–1289.

Yang, M.Y., Armstrong, J.D., Vilinsky, I., Strausfeld, N.J., and Kaiser, K. (1995). Subdivision of the *Drosophila* mushroom bodies by enhancer-trap expression patterns. Neuron *15*, 45–54.

Yao, T.P., Segraves, W.A., Oro, A.E., McKeown, M., and Evans, R.M. (1992). *Drosophila* ultraspiracle modulates ecdysone receptor function via heterodimer formation. Cell *71*, 63–72.

Yao, T.P., Forman, B.M., Jiang, Z., Cherbas, L., Chen, J.D., McKeown, M., Cherbas, P., and Evans, R.M. (1993). Functional ecdysone receptor is the product of EcR and Ultraspiracle genes. Nature *366*, 476–479.